

Rapid Communication

The clinical pathology of severe acute respiratory syndrome (SARS): a report from China

Yanqing Ding,* Huijun Wang, Hong Shen, Zhuguo Li, Jian Geng, Huixia Han, Junjie Cai, Xin Li, Wei Kang, Desheng Weng, Yaodan Lu, Dehua Wu, Li He and Kaitai Yao
Department of Pathology, Nan Fang Hospital, First Military Medical University, Guangzhou, Guangdong Province, 510515, PR China

*Correspondence to:

Dr Yanqing Ding, Department of Pathology, Nan Fang Hospital, First Military Medical University, Guangzhou, Guangdong Province, 510515, PR China.
E-mail: dyq@fimmu.com

Abstract

In order to investigate the clinical pathology of severe acute respiratory syndrome (SARS), the autopsies of three patients who died from SARS in Nan Fang Hospital Guangdong, China were studied retrospectively. Routine haematoxylin and eosin (H&E) staining was used to study all of the tissues from the three cases. The lung tissue specimens were studied further with Macchiavello staining, viral inclusion body staining, reticulin staining, PAS staining, immunohistochemistry, ultrathin sectioning and staining, light microscopy, and transmission electron microscopy. The first symptom was hyperpyrexia in all three cases, followed by progressive dyspnoea and lung field shadowing. The pulmonary lesions included bilateral extensive consolidation, localized haemorrhage and necrosis, desquamative pulmonary alveolitis and bronchitis, proliferation and desquamation of alveolar epithelial cells, exudation of protein and monocytes, lymphocytes and plasma cells in alveoli, hyaline membrane formation, and viral inclusion bodies in alveolar epithelial cells. There was also massive necrosis of splenic lymphoid tissue and localized necrosis in lymph nodes. Systemic vasculitis included oedema, localized fibrinoid necrosis, and infiltration of monocytes, lymphocytes, and plasma cells into vessel walls in the heart, lung, liver, kidney, adrenal gland, and the stroma of striated muscles. Thrombosis was present in small veins. Systemic toxic changes included degeneration and necrosis of the parenchyma cells in the lung, liver, kidney, heart, and adrenal gland. Electron microscopy demonstrated clusters of viral particles, consistent with coronavirus, in lung tissue. SARS is a systemic disease that injures many organs. The lungs, immune organs, and systemic small vessels are the main targets of virus attack, so that extensive consolidation of the lung, diffuse alveolar damage with hyaline membrane formation, respiratory distress, and decreased immune function are the main causes of death. Copyright © 2003 John Wiley & Sons, Ltd.

Received: 9 May 2003

Revised: 19 May 2003

Accepted: 19 May 2003

Introduction

An acute infectious disease spreading mainly via the respiratory route was first identified in Guangdong, China in November 2002 and was then found in other regions in Asia, North America, and Europe. In view of the clinical symptoms, the disease was initially referred to as 'atypical pneumonia' (AP). This disease has resulted in a severe epidemic outbreak in 27 countries and regions and it has been termed severe acute respiratory syndrome (SARS) by the World Health Organisation (WHO) [1–3]. Medical workers are at high risk of the disease. In this paper, we report the clinical pathology of three patients who died of SARS in Nan Fang Hospital, Guangzhou, Guangdong, PR China in early 2003.

Materials and methods

Clinical material

In early 2003, we collected data from the autopsies of three patients who died of SARS, one of whom

had a definite history of exposure to SARS. All three patients fulfilled the clinical case definition of SARS and the clinical details are listed in Table 1. There was no evidence of HIV infection, chronic lung disease, diabetes or malignancy in any of the patients. The families of the deceased gave consent to the autopsies, which were also approved by the medical administration.

Pathological examination and histochemical staining

Lung, liver, kidney, heart, brain, spleen, striated muscle, lymph node, bone marrow, and adrenal gland were collected. All specimens were fixed with 4% neutral formaldehyde, embedded in paraffin wax, and 4 µm sections were cut. Sections were stained with haematoxylin and eosin (H&E), Macchiavello's stain (for viral inclusion bodies), and reticulin.

Immunohistochemistry

A standard streptavidin peroxidase method was used. Cytokeratin (CK, 1 : 50), epithelial membrane antigen

(EMA, 1:100), CD68 (1:100), and leukocyte common antigen (LCA, 1:100) were all purchased from DAKO.

Transmission electron microscopy

Specimens from all three cases were fixed with 2.5% glutaraldehyde in phosphoric buffer, post-fixed with 1% osmate, dehydrated with gradient alcohol, embedded with Epon 812, double-stained with uranium acetate and lead citromalic acid, and observed under a JEM1200 transmission electron microscope.

Results

Clinical features

The onset of the disease in all cases was acute and sudden. The initial symptoms were related to pyrexia, followed by chills, generalized aching pains, non-productive cough, and sputum with a small quantity of blood (in one case). Chest radiographs showed patchy shadows in both lungs. The detailed data are listed in Table 1.

Macroscopic examination

At autopsy, there were no evident changes on the body surface except for scrotal oedema in one case. The predominant visceral macroscopic changes were enlargement of lymph nodes in the pulmonary hilar and

abdominal cavity to varying extents, diminished size of the spleen ($9.8 \times 5 \times 3$ cm, $8.2 \times 4.1 \times 2$ cm, and $7.4 \times 3.5 \times 2$ cm, respectively), and reduced weight of the spleen (110 g, 123 g, and 114 g, respectively). The spleens were soft and their capsules were shrunken. Extensive consolidation was present in the lungs (Figure 1). Dotted and patchy haemorrhage and necrosis could be seen on the surfaces and the cut sections of the lungs in two cases (A1 and A3) and the sections were red wine-coloured. Detailed thoracic macroscopic changes are listed in Table 2.

Microscopic examination

Lungs

The pulmonary changes were similar in all three cases. There was extensive bilateral consolidation, severe pulmonary oedema, and haemorrhagic infarction in two cases (A1 and A3). There was desquamative alveolitis and bronchitis, with proliferation and desquamation of alveolar epithelial cells (CK, EMA positive) (Figure 2), exudation of mononuclear cells, lymphocytes and plasma cells (CD68, LCA positive) (Figure 3), and alveolar oedema. The desquamated epithelial cells were clearly enlarged and some had undergone fusion to form syncytia. There were extensive hyaline membranes in alveoli (Figure 4). Focal necrosis with infiltration of neutrophils, monocytes,

Table 1. Clinical details

Case No	Gender	Age (years)	Duration of disease (days)	Temperature (°C)	Clinical symptoms and signs	White cell count and composition	Chest radiography
A1	Female	62	11	39.2	Headache, cough, chest pain, progressive dyspnoea	$5.98 \times 10^9/l$ Neutrophils 70.7% Lymphocytes 9.2%	Extensive shadowing in both lungs
A2	Male	25	10	39.6	Cough with blood-stained sputum	$6.03 \times 10^9/l$ Neutrophils 78.2% Lymphocytes 9.6%	Dense shadowing in right lung and upper part of left lung
A3	Male	57	20	39.8	Aching pains in whole body, dry cough, progressive dyspnoea, occasional moist rales in both lungs	$7.13 \times 10^9/l$ Neutrophils 64.9% Lymphocytes 8.4%	Extensive dense shadowing in both lungs

Table 2. Thoracic macroscopic changes

Case No	Pleural cavity	Pleura	Pulmonary artery	Lung	Cut surface of lung	Trachea
A1	Haemorrhagic fluid (250 ml)	Localized haemorrhage under pleura	Thrombus present	Bilateral consolidation	Red-coloured haemorrhagic infarct present	Focal haemorrhage in mucosa; turbid fluid in lumen
A2	Orange-coloured fluid (100 ml)	No evident changes	Thrombus present	Bilateral consolidation predominantly in lower lobes	Red-coloured fluid present	Congestion and focal haemorrhage in mucosa; pale red fluid in lumen
A3	Haemorrhagic fluid (400 ml)	Right pleural adhesions; focal sub-pleural haemorrhage	No thrombus present	Extensive bilateral consolidation	Focal haemorrhage; pale red fluid present	Focal haemorrhage and blood-stained purulent fluid in lumen



Figure 1. Gross morphology of the lung

and lymphocytes was present in all three cases. Intracytoplasmic viral inclusion bodies were seen in some alveolar epithelial cells. These were spherical, about the size of an erythrocyte, and acidophilic. They were surrounded by a hyaline halo (Figure 5) and were positive with Macchiavello's stain. Desquamation of bronchial epithelial cells was present and there was necrosis of some bronchial walls with infiltration of lymphocytes, monocytes, and neutrophils. The capillaries in interlobular septa and alveolar walls were dilated and congested. Most alveolar walls were not expanded (Figure 6A), but infiltration of monocytes and lymphocytes was present in a few widened alveolar walls and interlobular septa. In one case (A3), the alveolar exudates were organized and fibrosed (Figures 6B and 6C), while in the other two cases (A2 and A3), mononuclear and multinucleate giant cells

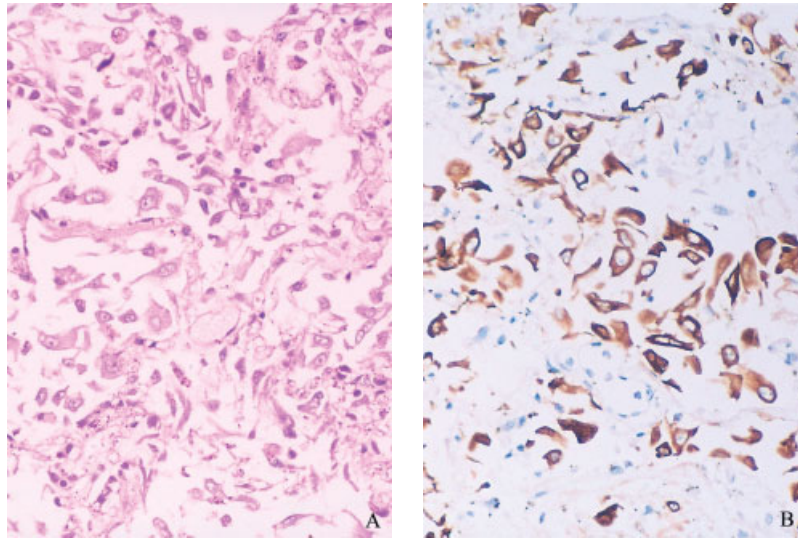


Figure 2. Alveoli filled with desquamated epithelial cells. (A) H&E (original magnification $\times 400$). (B) Cytokeratin (streptavidin peroxidase, original magnification $\times 400$)

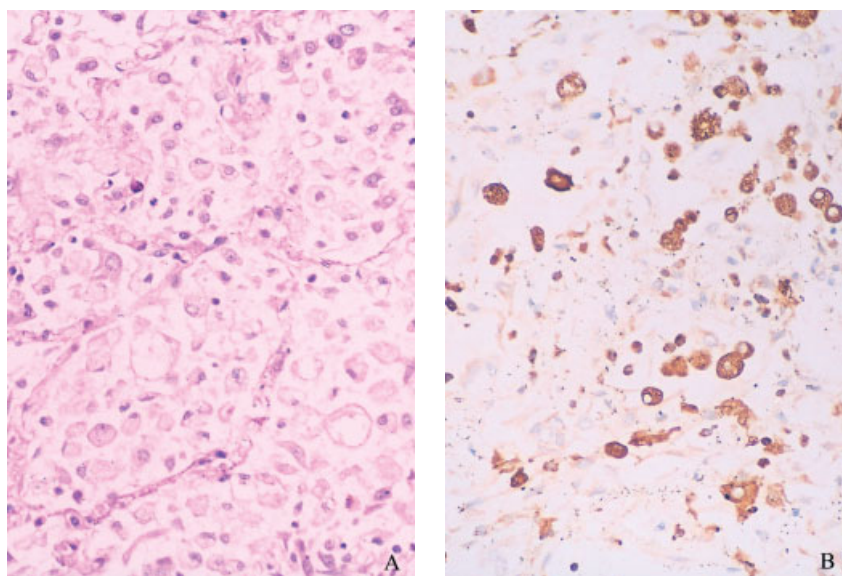


Figure 3. Exudation of monocytes into alveoli. (A) H&E, original magnification $\times 400$. (B) CD 68 (streptavidin peroxidase, original magnification $\times 400$)

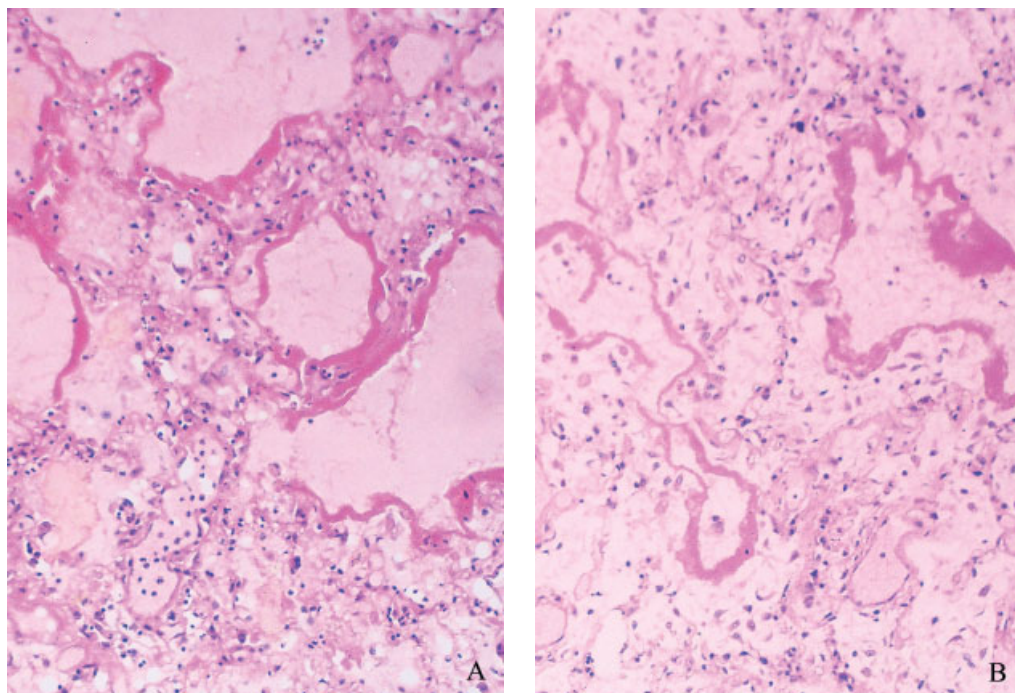


Figure 4. (A, B) Formation of hyaline membranes (H&E, original magnification $\times 200$)

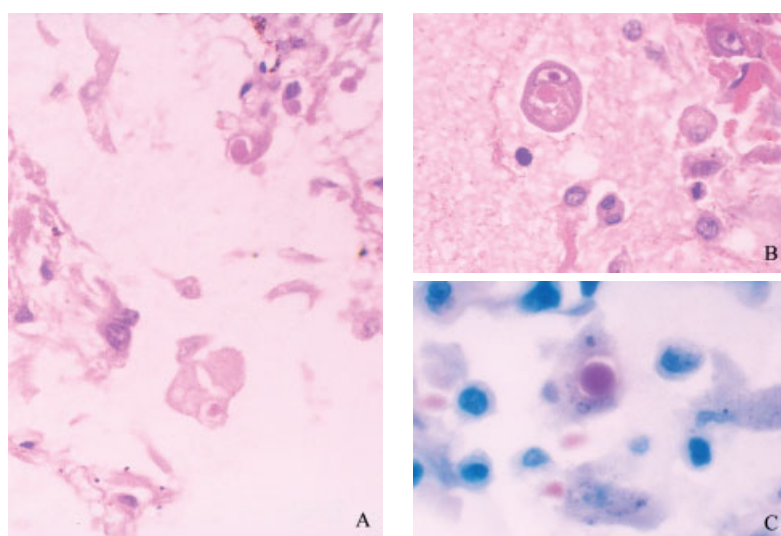


Figure 5. (A, B) Intracytoplasmic viral inclusion bodies in alveolar epithelial cells (H&E, original magnification $\times 400$). (C) Purple viral inclusion bodies (Macchiavello staining, original magnification $\times 1000$)

were seen in alveoli (Figures 7A–7C). The endothelial cells of small pulmonary veins were swollen and shed. Oedema was present in the walls of small veins and some veins showed fibrinoid necrosis with infiltration of monocytes, neutrophils, and lymphocytes. Mixed thrombi were present in small veins (Figure 8A) and hyaline thrombi appeared in microvessels. Overall, the pulmonary features were of diffuse alveolar damage causing acute respiratory distress syndrome.

Heart

There was myocardial stromal oedema. The endothelial cells of small veins were swollen and the vascular

walls were oedematous and infiltrated by monocytes and lymphocytes. There were focal hyaline degeneration and lysis of cardiac muscle fibres in one case (A1).

Spleen and lymph nodes

There was prominent splenic atrophy in all three cases, with massive necrosis of lymphoid tissue in white pulp and marginal sinus (Figures 9A and 9B). There was dilatation and congestion of vessels in pulmonary hilar and abdominal lymph nodes with loss of cortico-medullary distinction. The marginal sinus and germinal centres disappeared in some lymph nodes, and

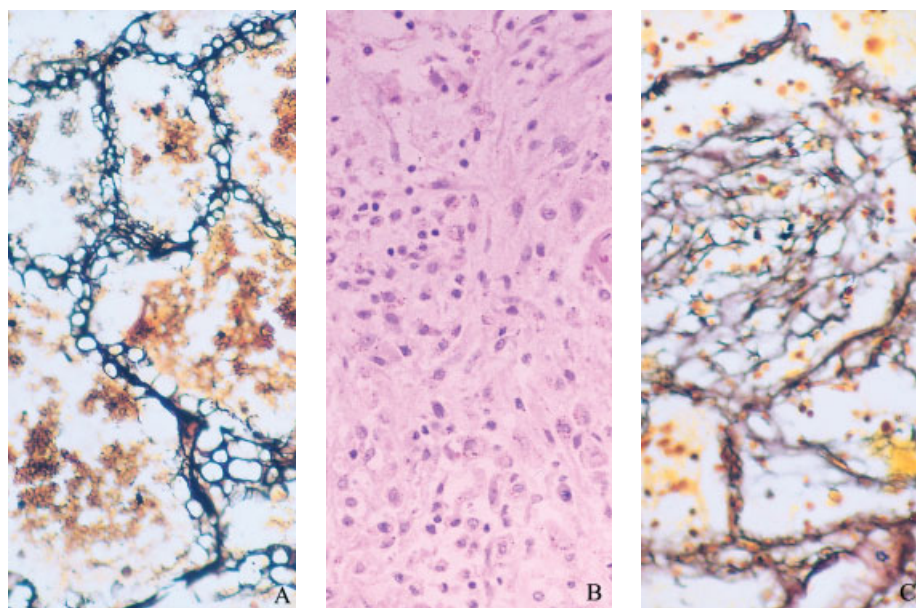


Figure 6. (A) There is no change in the width of the walls of abnormal alveoli (A_g, original magnification $\times 200$). (B) Organization of alveolar exudates (A₃, duration of 20 days) (H&E, original magnification $\times 200$). (C) Organization of alveolar exudates (A₃, duration of 20 days) (A_g, original magnification $\times 400$)

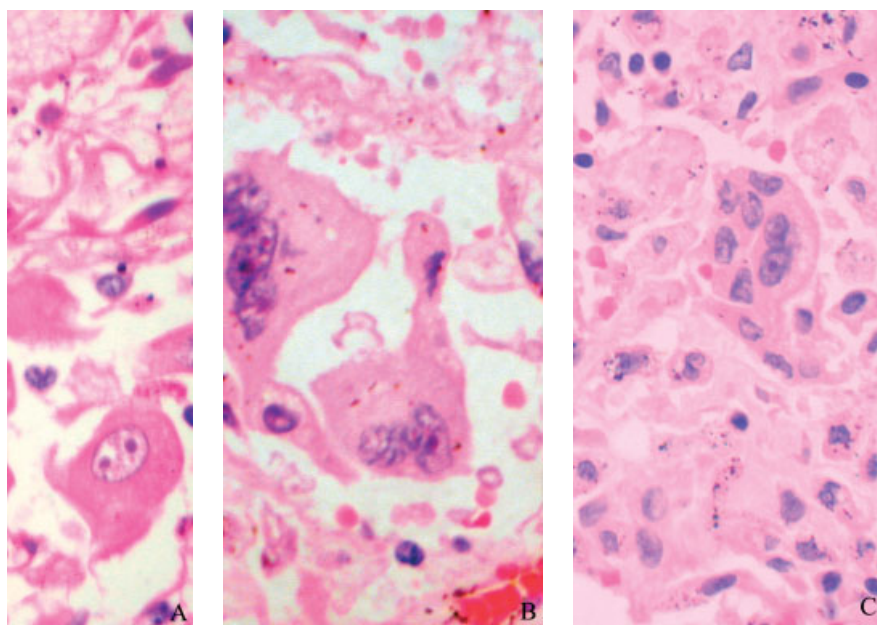


Figure 7. (A–C) Mononuclear and multinucleate epithelial giant cells in alveoli (H&E, original magnification $\times 540$)

many monocytes and plasmacytoid monocytes could be seen in the remaining lymphatic sinus. Localized necrosis was present and there was apoptosis of lymphocytes in both the spleen and the lymph nodes.

Liver

In one case (A₃), there was apparent dissociation of hepatocyte cords (Figure 10A), together with fatty degeneration and focal necrosis. In the other two cases (A₁ and A₂), the hepatocytes underwent massive central necrosis (Figure 10B). The vascular walls and circumference of small veins in the liver showed oedema and infiltration of monocytes and lymphocytes.

Kidney and adrenal glands

There was focal necrosis of the kidney and adrenal glands. Vasculitis of small veins in the renal interstitial tissue and medulla of the adrenal gland was present with associated infiltration chiefly of monocytes and lymphocytes.

Brain and muscle

In two cases (A₁ and A₂), there was oedema around the small veins in the brain, with infiltration of the vascular walls by monocytes and lymphocytes

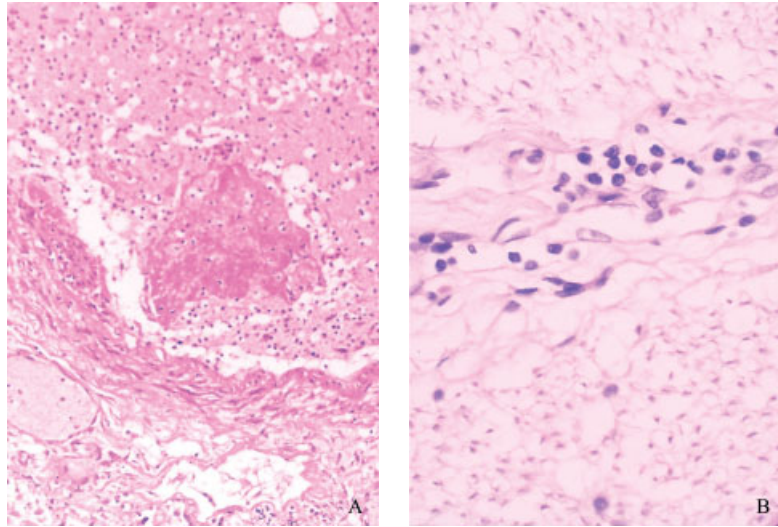


Figure 8. (A) Thrombosis and local necrosis of a vein wall in the lung (H&E, original magnification $\times 200$). (B) Vasculitis of small veins in the brain (H&E, original magnification $\times 200$)

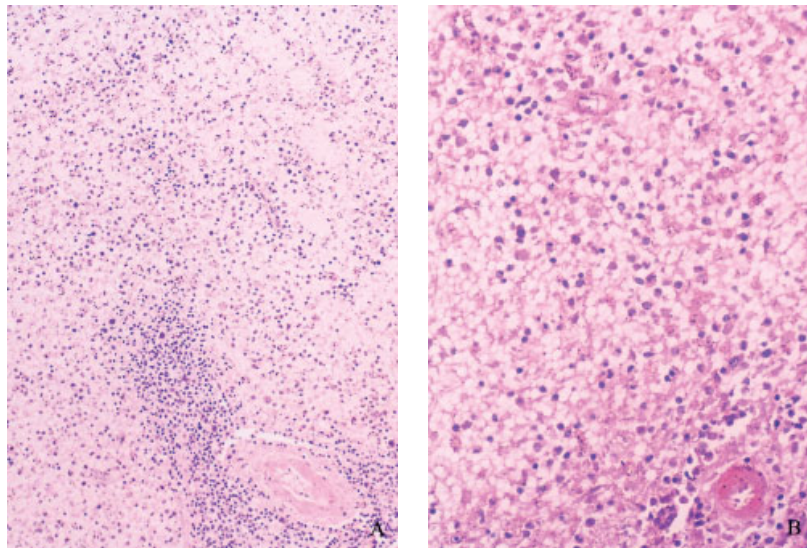


Figure 9. (A) Disappearance of a splenic corpuscle and (B) massive necrosis of lymphatic tissue (H&E, original magnification $\times 200$)

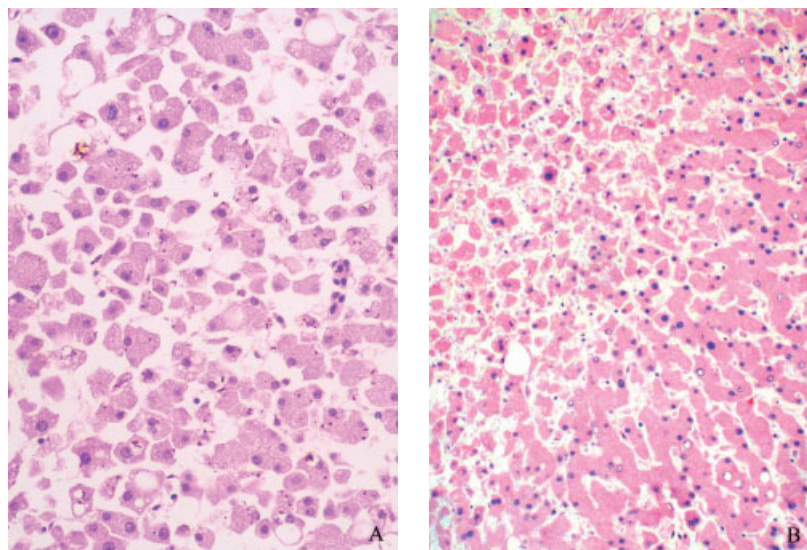


Figure 10. (A) Dissociation of hepatocyte cords. (H&E, original magnification $\times 400$). (B) Patchy necrosis of hepatocytes (H&E, original magnification $\times 200$)

(Figure 8B). The brain tissue was slightly oedematous, with demyelination of some nerve fibres and focal neuronal degeneration. The vessel walls and circumference of small veins and arteries in the striated muscles in the lower limbs showed oedema and infiltration of monocytes and lymphocytes.

Bone marrow

There was a decrease in bone marrow haematopoietic tissue, with a relative reduction in granulocyte megakaryocyte lineages and localized proliferation of polychromatophilic erythroblasts.

Transmission electron microscopy

Alveolar epithelial cells were markedly swollen, with expansion of mitochondria and expansion and vacuolation of the endoplasmic reticulum. There was hyperplasia of type 1 and type 2 epithelial cells, particularly type 2. The lamellar bodies in the cytoplasm of type 2 cells were either markedly reduced in number or absent. The rough endoplasmic reticulum (RER) and smooth endoplasmic reticulum (SER) proliferated and dilated greatly. In the dilated SER, there was exudation of protein with increased electron density. In a few dilated SER, there were clusters of viral particles 70–90 nm in diameter (Figure 11). In some nuclei, there were membranous inclusion bodies. The endothelial cells in the vessels of alveolar septa were swollen and vacuolated. There was exudation of some monocytes, lymphocytes, and plasma cells into the alveoli, but evidence of phagocytosis was absent in monocytes.

Discussion

SARS is an acute infectious disease that spreads mainly via the respiratory route. The first case was reported around Guangzhou, southern China, but as

the disease was unknown at this time, it resulted in severe infections of the medical personnel in the hospital, with an infection rate up to 33%. There has been a worldwide epidemic outbreak of SARS, since the disease is highly infectious, does not respond to conventional anti-microbial treatment, and has a high death rate. The WHO is taking urgent and co-operative action to combat this disease and important progress has been made in understanding its aetiology and epidemiology.

In this study, we report the detailed clinical pathology of three autopsy cases of SARS and provide findings that we hope will be helpful in understanding the nature of this disease. The onset of SARS is very acute and sudden. The initial symptom is fever, which is usually high or irregular. The patients may have minor symptoms suggestive of the common cold, such as chills, chest pain, and myalgia. They also have a non-productive cough and some may have traces of blood in their sputum. Neutropenia is typical. Dyspnoea is present and chest radiography shows localized or diffuse shadowing which may be progressive. In some patients, the clinical symptoms are inconsistent with the degree of pulmonary involvement, in that while their clinical symptoms appear slight, their lung lesions deteriorate progressively.

With regard to the aetiology and pathogenesis of SARS, this study has demonstrated extensive pulmonary consolidation; significant pulmonary oedema; localized haemorrhage and necrosis; widespread hyaline membrane formation; a local inflammatory reaction consisting mostly of monocytes, lymphocytes, and plasma cells; desquamation of bronchial and alveolar epithelial cells; numerous multinucleate and mononuclear giant cells in pulmonary alveoli in two cases; and typical viral inclusion bodies in epithelial cells in alveoli in all the three cases. Viral particles were identified by transmission electron microscopy. Analysing research findings from several countries, the WHO has declared that the likely pathogen is a variant of

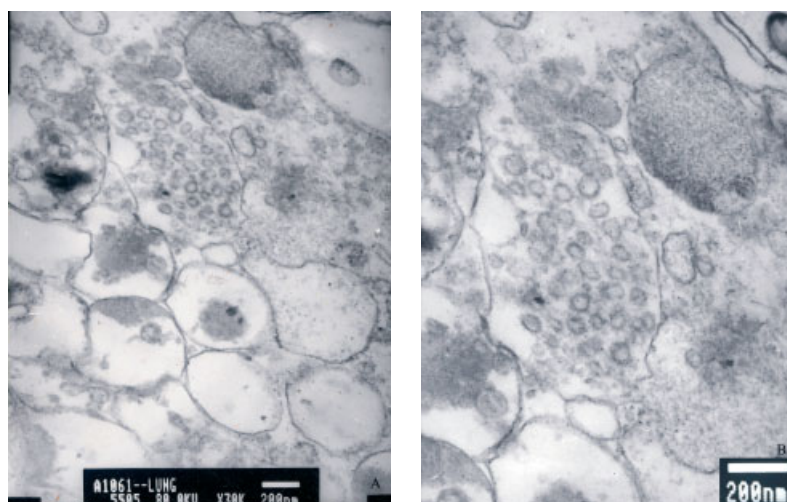


Figure 11. (A) Dilatation of SER and clusters of viral particles in smooth endoplasmic reticulum of type 2 alveolar pneumocyte (bar = 500 nm). (B) Amplified clusters of viral particles shown in A (bar = 200 nm)

coronavirus (CV) and has named it the SARS virus [4]. The viral particles and viral inclusion bodies observed by electron microscopy and light microscopy, respectively, in this study are of a similar size and morphological form to those of the SARS virus and our findings therefore support the association of the SARS coronavirus with the pathogenesis of this disease. Although it is a variant of CV, the SARS virus has the same virological characteristics as CV. It is an RNA virus, the membrane of which contains two types of glycoprotein, E1 and E2, which bind to the receptors of the sensitive cells and enter by endophagocytosis, replicating entirely in the cytoplasm [5]. Recent studies indicate that the cellular receptors for CV (CD₁₃) exist predominantly in mononuclear cells, venular endothelial cells, epithelial cells in the respiratory tract and renal tubules, fibroblasts, brush-border cells of the intestine, stromal cells in the bone marrow, and the synaptic membrane of the central nervous system. We also found that pulmonary alveolar epithelial cells (mainly type 2) and epithelial cells in bronchi proliferated and desquamated, so that desquamative pulmonary alveolitis and bronchitis occurred. Endothelial cells in the systemic venules also desquamated and an inflammatory reaction was present in blood vessel walls (vasculitis). Degenerative changes, apoptosis, and necrosis occurred in parenchymal organs and tissue. We believe that all of these changes most likely result from a complicated process involving (1) disturbed cell metabolism as a result of the release of a large number of viral particles following entry into sensitive cells and rapid replication; (2) intense local vascular reactions; and (3) immune impairment mediated by cellular immunity and cytokine functions [6]. This conclusion requires confirmation through additional research.

The main pathological changes involve the lungs. Bilateral extensive consolidation of the lungs results from a combination of the large number of desquamated and exudated cells and protein exudates that congest the lung tissues, and the extensive formation of hyaline membranes in the alveoli. The pathology is essentially that of diffuse alveolar damage with subsequent progression to acute respiratory distress syndrome. From a clinical point of view, the patients exhibit worsening dyspnoea and die of respiratory failure.

The pathological changes of SARS can be summarized in terms of the following four aspects: pulmonary lesions; lesions of immune organs; systemic vasculitis; and systemic toxic reactions. The pulmonary lesions mainly involve alveoli and are chiefly composed of

desquamative pulmonary alveolitis and bronchitis, for no significant changes in width were observed in most of the alveolar walls or interlobular septa. Other lesions are formation of hyaline membranes, massive exudation of inflammatory cells into alveoli, patchy haemorrhage and focal necrosis, and organization of exudates in the alveoli in patients with a prolonged disease course (A3, 20 days). The main lesions of immune organs are massive necrosis in the spleen and local necrosis in lymph nodes. Systemic vasculitis involves proliferation, swelling, and apoptosis of endothelial cells, with infiltration of monocytes, lymphocytes, and plasma cells both around the circumference of small veins and in vascular walls in the heart, lung, liver, kidney, adrenal gland, and the interstitium of striated muscle. Fibrinoid necrosis and thrombosis occurred in parts of small veins. Systemic toxic changes included degeneration and necrosis of the parenchyma cells in the lung, liver, kidney, heart, and adrenal gland, as well as degeneration of nerve cells in the brain. It is most probable that these systemic reactions are related to viraemia.

In conclusion, we consider that SARS is a viral disease that can result in injury to multiple organs, although the predominant pathology involves the lungs.

Acknowledgements

Yanqing Ding acknowledges the permission of the Health Administration of Guangdong Province, PR China, the Eighth People's Hospital, Guangzhou City, and the Second Affiliated Hospital of Zhongshan University to carry out this study and the careful revision of the English version by Professor Liang Ping. Grants from National and Guangdong Specialized Funds are also acknowledged.

References

1. Update: Outbreak of severe acute respiratory syndrome-worldwide. *Morb Mortal Wkly Rep* 2003; **52**(11): 241–248.
2. Tsang KW, Ho PL, Ooi GC, *et al.* A cluster of cases of severe acute respiratory syndrome in Hong Kong. *N Engl J Med* 2003; **348**: 1–9 (published at www.nejm.org. [31 March 2003]).
3. Poutanen SM, Low DE, Henry B, *et al.* Identification of severe acute respiratory syndrome in Canada. *N Engl J Med* 2003; **348**: 1–11 (published at www.nejm.org. [31 March 2003]).
4. Thomas G, Ksiazek D, Erdman D, *et al.* A novel coronavirus associated with severe acute respiratory syndrome. *N Engl J Med* 2003; **348**(20): 1953–1966.
5. Luby JP, Clinton R, Kurtz S. Adaptation of human enteric coronavirus to growth in cell lines. *J Clin Virol* 1999; **12**: 43–51.
6. Yeager CL, Ashmun RA, Williams RK, *et al.* Human aminopeptidase N is a receptor for human coronavirus 229E. *Nature* 1992; **357**: 420–422.